



CHORUS

This is the accepted manuscript made available via CHORUS. The article has been published as:

Transition from Continuous to Discontinuous Shear Thickening: An Excluded-Volume Effect

Yasaman Madraki, Guillaume Ovarlez, and Sarah Hormozi

Phys. Rev. Lett. **121**, 108001 — Published 5 September 2018

DOI: [10.1103/PhysRevLett.121.108001](https://doi.org/10.1103/PhysRevLett.121.108001)

Transition from Continuous to Discontinuous Shear Thickening: An Excluded Volume Effect

Yasaman Madraki¹, Guillaume Ovarlez², Sarah Hormozi^{1*}

¹*Department of Mechanical Engineering, Ohio University, Athens, Ohio 45701-2979, USA*

²*University of Bordeaux, CNRS, Solvay, LOF, UMR 5258, 33608 Pessac, France*

(Dated: July 27, 2018)

In this letter, we present a new mechanism under the action of which a shear thickening suspension transitions from a continuous to a discontinuous regime. This transition occurs by adding high concentrations of large spheres to a continuous shear thickening suspension. We show that the solid volume fraction of the interstitial shear thickening matrix is locally enhanced due to the presence of large particles and the excluded volume shells surrounding the large particles. Thus leading to a continuous to discontinuous shear thickening transition at the local scale.

Shear thickening is defined as a viscosity increase with increasing applied shear stress or shear rate [1–3]. **Shear thickening suspensions are broadly found in nature and industry, with applications in dampening and shock absorption, such as found in armor composite material [4] and curved-surface shear-thickening polishing [5].** Therefore, the understanding and control of their rheological behavior would help in solving the current problems or create opportunities for innovative technological ideas inspired by this behavior. The thickening regime might be observed as a smooth increase of the viscosity with the shear rate known as the Continuous Shear Thickening (CST). It can also be observed as an abrupt increase up to some degree of magnitude at a specific shear rate, $\dot{\gamma}_{critical}$, known as Discontinuous Shear Thickening (DST). These two different thickening regimes are both spectacularly observed in cornstarch suspension at different cornstarch concentrations. The nature of shear thickening behavior has been debated for many years, but the theory of the transition from a frictionless to a frictional state of the suspension [6–9] has been recently validated by experimental results [10–15]. The shear thickening behavior is reported in the mono-dispersed, bi-dispersed and polydispersed suspensions [16–18] which are made of Brownian [1] or non-Brownian [19] particles.

It has been shown that adding large particles to a fluid enhances both the effective viscosity of the bulk and the local shear rate of the fluid phase. While the latter has no influence on the viscosity of Newtonian suspending fluids, it strongly influences the local apparent viscosity in the case of generalized Newtonian suspending fluids. A number of experimental works have been carried out, see e.g., [16, 17, 20–27], to study the bulk rheology of particles suspended in generalized Newtonian suspending fluids following the power law or Herschel-Bulkley models. The results show that the bulk rheology of suspensions follow the rheology model of the interstitial suspending fluids, but with a yield stress and a consistency that increase with the solid volume fraction. This rheological enhancement is also observed when we add large particles to a CST or a DST suspension, i.e., the apparent viscosity enhances and the onset of CST or DST advances [17, 18]. In all of these scenarios, the rheological behavior of the system (e.g., CST, DST or yield stress behavior) remains invariant after adding large particles to it. The homogenization approach

is adopted to formulate constitutive laws for suspensions of non-Brownian particles in generalized Newtonian fluids [20].

In this paper, we show that adding large spheres to a CST cornstarch suspension can lead to a transition from CST to DST at high concentrations of large spheres. This transition from one rheological behavior to another, i.e., the CST behavior to the DST behavior, cannot be explained by current theories [20] and has not yet been reported experimentally. **We propose an underlying mechanism for this transition stemming from geometrical constraints in bi-disperse suspensions, the large particles introducing an inaccessible volume to cornstarch grains resulting in a change of the local volume fraction. This concept of excluded volume is thus shown here to have a new application in non-Brownian suspensions, in addition to the various phenomena already evidenced in colloidal systems where it is at the origin of entropic depletion interactions [28], and has more generally an impact on the suspensions structure. It leads to, e.g., isotropic to nematic transition in suspensions of rods [29] and is used to direct particle self assembly [30, 31] to design smart materials.**

The system of study consists of large particles in a shear thickening suspension made of cornstarch grains (73% amylopectin and 27% amylose from Sigma Aldrich, USA) and an aqueous solution, the micrograph is shown in Fig. 1b. The irregular shaped cornstarch grains with a density of 1.68 g/cm^3 are in size range of $5 - 20 \mu\text{m}$ with an average size of $d_{cs} = 15 \mu\text{m}$ (measured after analyzing a hundred of micrograph images). The aqueous solution consists of 54 wt% Cesium Chloride (Cabot high-purity grade from Sigma Aldrich, USA) dissolved in distilled water solvent. The large particles are polymethyl methacrylate (PMMA) spheres (Cospheric, USA) coated with silver, providing a density of 1.34 g/cm^3 as close as possible to the cornstarch suspension. We have used three different sizes of large particles within diameter ranges of $45 - 53 \mu\text{m}$, $106 - 125 \mu\text{m}$ and $125 - 135 \mu\text{m}$. These large particles have respectively the following average diameter size of $d_p = 49 \mu\text{m}$, $d_p = 115.5 \mu\text{m}$ and $d_p = 130 \mu\text{m}$. It should be noted that the suspension of these large particles in an aqueous solution, with concentration range used in this paper, do not exhibit any shear thickening behavior. Therefore, our system is a mixture of thickening (cornstarch) and non-thickening (PMMA) particles. The cornstarch suspension with a volume fraction ϕ_{cs} is prepared via $\phi_{cs} = V_{cs}/(V_{cs} + V_{aq})$, where V_{cs} ,

V_{aq} are the volume of cornstarch grains and aqueous solution respectively. Large particles are then added into this suspending medium with volume fraction $\phi_p = V_p/V_t$, where V_p is the volume of particles and V_t is the total volume of the suspension as $V_t = V_p + V_{cs} + V_{aq}$.

The rheological experiments are performed using a DHR-3 rotational rheometer (TA Instruments). We use a parallel plate geometry with a diameter of $2R = 40 \text{ mm}$ and a rough pattern of V-shaped grooves with a 90 deg angle, a height of 0.5 mm and a width of 1 mm , see Fig. 1a. This geometry allows us to avoid the wall slip effect. The gap between the plates is $h = 1.5 \text{ mm}$. We have checked our measurements to be independent of the gap size for $750 \mu\text{m} \leq h \leq 2500 \mu\text{m}$. We also use a smooth parallel plate geometry with a diameter of 60 mm . This second geometry is used for the experiments performed at various gap sizes to simulate the excluded volume effect, explained later. The rheological measurements consist of performing an increasing logarithmic shear rate ramp and determining the shear stress τ , normal stress difference $N = N_1 - N_2$ and the viscosity η . A sweep time of $t = 180$ seconds and a resolution of 100 data/decade are chosen for most of the experiments. Our measurements are consistent and not affected by sedimentation and evaporation for a range of sweep times between 120 s and 300 s . In addition, we have checked that our measurements are reproducible. It is noteworthy to mention that for each data point, we report the maximum values of shear rate $\dot{\gamma} = \Omega R/h$ and stress $\tau = 2C/\pi R^3$ occurring at the edge of the parallel plate geometry and we subtract inertial thrust from N values [32].

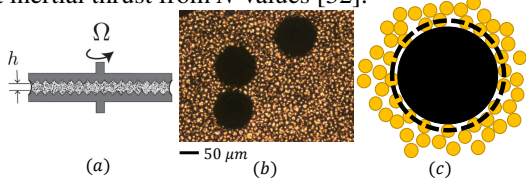


FIG. 1: (a) Sketch of the parallel plate geometry exhibiting the manufactured pattern. (b) Micrograph of silver-coated PMMA particles (large black spheres) and cornstarch grains (small grains). (c) Sketch of a large particle (large black sphere) in cornstarch (small grains) suspension and the excluded volume shell surrounding it in the bi-dispersed system.

Fig. 2a & b show the rheometry results of η and N versus $\dot{\gamma}$ for the suspension of cornstarch at various volume fractions, $0.345 \leq \phi_{cs} \leq 0.39$. The cornstarch suspension exhibits a CST behavior when $\phi_{cs} \lesssim 0.38$ and transitions to a DST for larger values of ϕ_{cs} . This transition from the CST to DST is accompanied by a change of sign in N . **We add large particles with diameter size of $d_p = 115.5 \mu\text{m}$** to two suspensions of cornstarch with $\phi_{cs} = 0.30$ (Fig. 2 c & d) and $\phi_{cs} = 0.345$ (Fig. 2 e & f), which both initially exhibit CST behaviors. We observe that as we increase the volume fraction of large particles, ϕ_p , the viscosity of suspension increases and the onset of CST expedites to the smaller values of shear rates. This enhancement in the thickening behavior is consistent with previous observations [16, 18] which is due to the change in the

relative viscosity and local shear rate owing to the fact that large particles are not deformable [17, 25, 33]. Remarkably, we observe that as we enlarge ϕ_p at certain values ($\phi_p = 0.35$ in Figs. 2c & d and $\phi_p = 0.20$ in Figs. 2e & f) the rheology transitions from one behavior to another, i.e., CST to DST, identified by a jump in the viscosity (Fig. 2c & e) and the change in the sign of N (Fig. 2d & f). Note that the data obtained after the occurrence of DST are not reliable since fracturing and ejection of the material are observed at the edge of the parallel plate geometry. This phenomenon cannot be rationalized by the previous framework [17, 25, 33]. The reason is that large particles are not deformable which it only affects the values of local shear rate. As we have shown in Fig. 2a & b, transitioning from the CST to DST behavior is controlled by the values of the cornstarch volume fraction and not the shear rate. Therefore, adding large particles should result in a mechanism under the action of which the volume fraction of cornstarch, ϕ_{cs} , enhances. This leads to a drastic change of the rheological behavior from the CST to DST.

Due to the presence of large particles in the cornstarch suspension, the cornstarch grains cannot come closer than their radius to the surface of the large particles (Fig. 1c). Therefore there exist shells mostly composed of the aqueous solution surrounding the large particles. As a result, the cornstarch concentration locally decreases in these shells at the surface of the large particles, which should be compensated by an increase of ϕ_{cs} elsewhere. This might lead to creating zones with larger values of cornstarch concentration where the cornstarch suspension goes into the DST regime. The effective cornstarch concentration, denoted by ϕ_{cs}^e , in these regions can be estimated via the following procedure. We estimate the volumes of the aqueous shells as $V_s = \phi_p V_t ((d_p + d_{cs})^3 - d_p^3)/d_p^3$ and exclude it from the volume of the aqueous solution, which is $V_{aq} = (1 - \phi_{cs})(1 - \phi_p)V_t$. This corrected aqueous solution is denoted by V_{aq}^c and used to calculate the effective cornstarch concentration as $\phi_{cs}^e = V_{cs}^c/(V_{cs} + V_{aq}^c)$. This purely geometrical mechanism, hereafter excluded volume effect, suggests that excluding the volumes of shells from the total volume of aqueous solution leads to an effective cornstarch volume fraction ϕ_{cs}^e in our bi-dispersed system of suspensions. The ϕ_{cs}^e depends on the bulk cornstarch volume fraction, ϕ_{cs} , the volume fractions of large particles and their sizes. We hypothesize that the value of ϕ_{cs}^e determines the transition from CST to DST. To test this hypothesis, we perform a series of experiments based on an experimental matrix designed as follows. First, we plot the colormap of ϕ_{cs}^e in the plane of ϕ_{cs} and ϕ_p for a fixed average size of large particles, e.g., $d_p = 115.5 \mu\text{m}$ in Fig. 3(a). Then, we overlap on this map the iso-line of $\phi_{cs}^e = 0.38$ corresponding to the CST to DST transition for the pure cornstarch suspension (as indicated in Fig. 2(a)). This iso-line divides the colormap into two regions. Based on our hypothesis, below the iso-line we should observe the CST behavior since $\phi_{cs}^e < 0.38$ while above the iso-line we should observe the DST behavior since $\phi_{cs}^e > 0.38$. We perform a series of rheometry tests for a range of ϕ_{cs} and ϕ_p to show that our bi-dispersed system of suspension transitions from CST

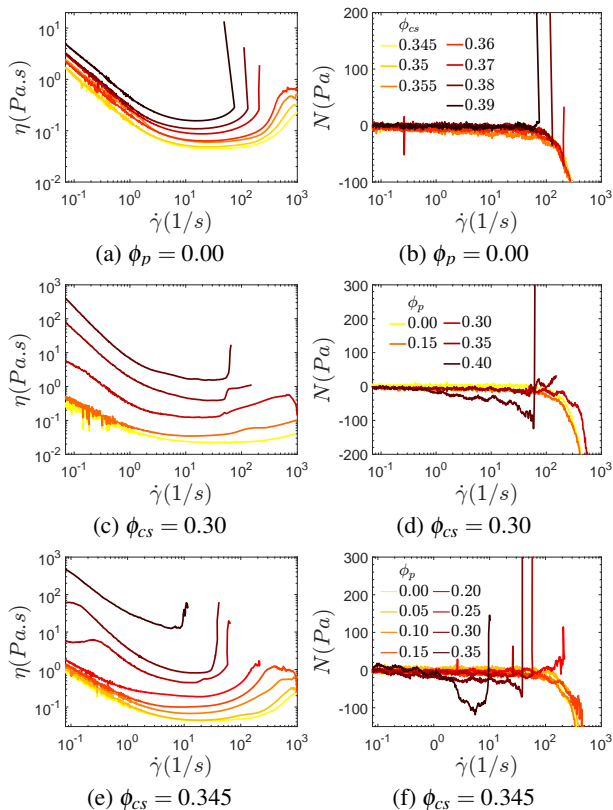


FIG. 2: Viscosity η ($Pa.s$) (left column of figure) and normal stress difference N (Pa) (right column of figure) vs shear rate $\dot{\gamma}$ ($1/s$) for: (a),(b) pure cornstarch suspensions at different ϕ_{cs} . (c),(d) mixtures of silver-coated PMMA particles, $d_p = 115.5 \mu m$, and a cornstarch suspension at $\phi_{cs} = 0.30$ for different particle volume fraction ϕ_p exhibiting a transition from CST to DST at $\phi_p = 0.35$. (e),(f) mixtures of silver-coated PMMA spheres, $d_p = 115.5 \mu m$, and a cornstarch suspension at $\phi_{cs} = 0.345$ for different particle volume fraction ϕ_p exhibiting a transition from CST to DST at $\phi_p = 0.20$.

to DST as soon as we pass the iso-line of $\phi_{cs}^e = 0.38$. Fig. 3(b) shows a typical example of our results in the plane of η vs $\dot{\gamma}$. We start with the pure cornstarch suspension with $(\phi_{cs}^e, \phi_{cs}, \phi_p) = (0.345, 0.345, 0.00)$ and we map the properties of this suspension on the colormap in Fig. 3(a) denoted by an open circle (1). The rheometry result associated with this suspension is shown in Fig. 3(b), see curve (1). The suspension exhibits the CST behavior when $\dot{\gamma} \gtrsim 100$. We add large particles into this pure cornstarch suspensions and perform the rheometry. We observe that when $\phi_{cs}^e < 0.38$, e.g., suspensions shown by open circles (2), (3) & (4) in Fig. 3(a), rheometry results indicate the CST behavior, see associated rheometry curves (2), (3) & (4) in Fig. 3(b). However, for those suspensions with $\phi_p \geq 0.20$ the effective cornstarch volume fraction exceeds 0.38, see e.g., points (5), (6), (7), & (8) shown by solid circle in Fig. 3(a), and consequently the suspensions exhibit DST as shown by curve (5), (6), (7), & (8) in

Fig. 3(b). Although for all data points (1)-(8) the bulk volume fraction of cornstarch is constant ($\phi_{cs} = 0.345$), the effective cornstarch volume fraction varies and increases with ϕ_p leading to the DST behavior as it exceeds 0.38, i.e., the approximate critical volume fraction of pure cornstarch at which DST occurs. It should be noted that in the calculations the excluded volume is estimated for dilute cornstarch suspensions, and the volume of water considered is likely exaggerated due to cornstarch grains' irregular shape and poly-dispersity. This estimation thus probably gives us larger effective cornstarch concentration than the real number. Therefore, it explains why transitions from CST to DST occur at $\phi_{cs}^e = 0.38$ instead of $\phi_{cs}^e = 0.37$ (expected from the rheometry of pure cornstarch suspension, Fig. 2(a) & (b)).

We have studied the rheological behavior of more suspensions with different values of bulk cornstarch concentration in the range of $0.28 < \phi_{cs} < 0.36$, large particles' volume fraction in the range of $0 < \phi_p < 0.4$ and large particles average diameter in the range of $49 \mu m < d_p < 130 \mu m$. Our results show that for those suspensions with $\phi_{cs}^e < 0.38$, shown as open circles in Fig. 3(a) & (d), the rheology exhibits the CST, while for those suspensions with $\phi_{cs}^e > 0.38$ shown as solid circles in Fig. 3(a) & (d), the rheology exhibits the DST. The rheometry results for some of these suspensions are shown in Fig. 3(b), (c), (e) & (f). We also performed the same experiments with shear stress controlled ramps and we obtained the same results. In addition, we performed the experiments using large particles, made of PMMA without silver coating, and the same transition was observed as well.

In order to further validate our analysis, we have studied viscometric flows of a cornstarch suspension between two smooth plates. The idea is to force the particle to adopt the same structure close to the smooth plate as that close to the surface of large particles. As we increase the volume fraction of large particles in our system of suspensions, the value of mean surface-to-surface distance of large particles decreases. This results in confining the cornstarch suspensions, which itself enhances the excluded volume effect leading to a larger ϕ_{cs}^e . The same flow scenario can be created by decreasing the gap between two parallel plates to confine the cornstarch suspension. The excluded volume is expected to have increasing importance as we decrease the gap, leading to a significant increase of the effective cornstarch volume fraction away from the parallel plate boundaries. Therefore, we expect a suspension, which initially exhibits the CST behavior, to transition to DST as we decrease the gap. We note that the shear thickening enhancement in CST colloidal suspension has already been demonstrated by narrow gap Couette measurements [34] and simulations [35]. However, there exists no study on the novel phenomenon of transition from CST to DST due to the confinement or equivalently excluded volume effect. The excluded volume in our rheometry tests includes the volume of two cylindrical shells, $V_s = 2\pi R^2(d_{cs}/2)$, each with a radius equal to that of the parallel plates and a height equal to the mean radius of the cornstarch grain $d_{cs}/2$. Subtracting V_s from the total amount of aqueous solution loaded be-

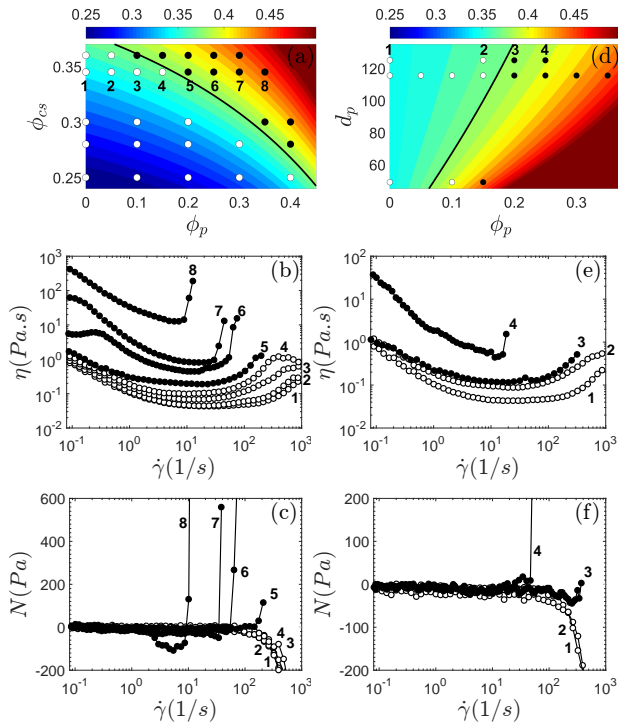


FIG. 3: (a) Color map of effective cornstarch volume fraction ϕ_{cs}^e in the plane of bulk cornstarch volume fraction ϕ_{cs} and large particles volume fraction ϕ_p for $d_p = 115.5 \mu m$. Black solid line corresponds to $\phi_{cs}^e = 0.38$. The data points are shown as open circles and solid circles, corresponding to the experiments exhibiting CST and DST behavior, respectively. The rheometry results are provided for those numbered symbols in the following sub-figures: (b) Viscosity η (Pa.s) and (c) normal stress difference N (Pa) vs shear rate $\dot{\gamma}$ (1/s) for the numbered experimental data in (a): $d_p = 115.5 \mu m$, $\phi_{cs} = 0.345$. (d) Color map of effective cornstarch volume fraction ϕ_{cs}^e in the plane of bulk cornstarch volume fraction, d_p and large particles, silver-coated PMMA, volume fraction ϕ_p for $\phi_{cs} = 0.345$. Black solid line corresponds to $\phi_{cs}^e = 0.38$. The data points are shown as open circles and solid circles, corresponding to the experiments exhibiting CST and DST behavior, respectively. The rheometry results are provided for those numbered symbols in the following sub-figures: (e) Viscosity η (Pa.s) and (f) normal stress difference N (Pa) vs shear rate $\dot{\gamma}$ (1/s) for the numbered experimental data in (d): $d_p = 130 \mu m$, $\phi_{cs} = 0.345$

◊ ◊ ◊

tween the gap gives us the effective cornstarch volume fraction, $\phi_{cs}^e = V_{cs}/(V_{cs} + V_{aq} - V_s) = \phi_{cs}h/(h - d_{cs})$.

We perform rheometry tests on a CST cornstarch suspension, with $\phi_{cs} = 0.345$, sandwiched between smooth parallel plates. We correct our results at very small gaps taking into account the surface roughness and possible misalignments of the parallel plates [32]. The results are shown in the plane of η vs $\dot{\gamma}$ in Fig. 4(a) and in the plane of N vs $\dot{\gamma}$ in Fig.

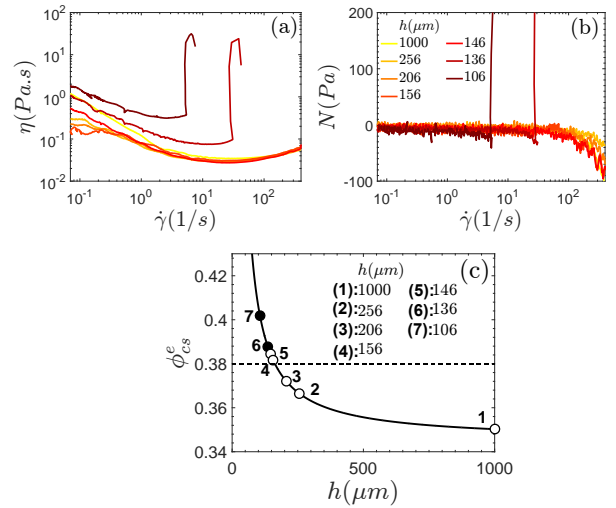


FIG. 4: (a) Viscosity η (Pa.s) and (b) normal stress difference N (Pa) vs shear rate $\dot{\gamma}$ (1/s) for different gap sizes h (μm) with a cornstarch suspension at $\phi_{cs} = 0.345$ exhibiting the transition from CST behavior to DST behavior at narrow gap sizes. (c) Effective cornstarch volume fraction ϕ_{cs}^e vs the gap size h (μm). The data points are shown as open and solid circles, corresponding to the curves in (a) and (b) exhibiting CST and DST behavior, respectively.

4(b). We observe that as the gap size is decreased, the CST behavior enhances and at a gap size of $h = 136.06 \mu m$ the cornstarch suspension transitions to the DST, which is accompanied by a discontinuous jump in η (Fig. 4(a)) as well as the change of sign in N (Fig. 4(b)). In these experiments, the wall slip is negligible [36] considering small viscosity behavior change at low shear rates when we decrease the gap size from $1000 \mu m$ to $200 \mu m$ compared to the drastic change we observe Fig. 4(c) shows the plot of ϕ_{cs}^e vs h when $\phi_{cs} = 0.345$. We also show in Fig. 4(c) the tests exhibiting CST by open circles and the tests exhibiting DST by solid circles. Based on our hypothesis, the transition to the DST should occur when $\phi_{cs}^e = 0.38$, which is at $h = 163 \mu m$. We observe that our results are in agreement with our hypothesis.

In this letter, we show that adding large particles to a shear thickening suspension containing small grains might lead to a drastic change in the rheological behaviors, i.e., transitioning from the CST to DST. This novel phenomenon is due to the presence of geometrical constraints in bi-disperse systems. More precisely, large particles displace centers of small particles and locate them at closest in a shell with a thickness of the order of radius of small grains. This results in a variation of the local volume fraction of the small grains, creating zones with the larger concentration that might undergo a DST behavior. As the result of this effect, controlling variables of d_p , ϕ_p and ϕ_{cs} in a suspension would be a promising method to engineer a suspension with desired shear thickening response based on the calculated effective cornstarch volume fraction.

S.H. acknowledges the financial support of NSF Grant No. CBET-1554044-CAREER. G.O. acknowledges the support of

the French Agence Nationale de la Recherche (ANR), under grant ANR-17- CE07-0040-05 (project FLUIDIDENSE). We thank Dr. David F. J. Tees (Department of Physics and Astronomy, Ohio University) for his assistance on the suspension micrography. We thank Aaron Oakley for his help in designing the suspensions. We also acknowledge the Kavli Institute for Theoretical Physics for hospitality during the discussion and write up of this manuscript.

* hormozi@ohio.edu

- [1] H. Barnes, *Journal of Rheology* **33**, 329 (1989).
- [2] J. Mewis and N. J. Wagner, *Colloidal suspension rheology* (Cambridge University Press, 2012).
- [3] E. Brown and H. M. Jaeger, *Reports on Progress in Physics* **77**, 046602 (2014).
- [4] Y. S. Lee, E. D. Wetzel, and N. J. Wagner, *Journal of materials science* **38**, 2825 (2003).
- [5] M. Li, B. Lyu, J. Yuan, C. Dong, and W. Dai, *International Journal of Machine Tools and Manufacture* **94**, 88 (2015).
- [6] C. Heussinger, *Physical review E* **88**, 050201 (2013).
- [7] R. Seto, R. Mari, J. F. Morris, and M. M. Denn, *Physical review letters* **111**, 218301 (2013).
- [8] M. Wyart and M. Cates, *Physical review letters* **112**, 098302 (2014).
- [9] R. Mari, R. Seto, J. F. Morris, and M. M. Denn, *Journal of Rheology* **58**, 1693 (2014).
- [10] B. Guy, M. Hermes, and W. Poon, *Physical review letters* **115**, 088304 (2015).
- [11] N. Y. Lin, B. M. Guy, M. Hermes, C. Ness, J. Sun, W. C. Poon, and I. Cohen, *Physical review letters* **115**, 228304 (2015).
- [12] M. Hermes, B. M. Guy, W. C. Poon, G. Poy, M. E. Cates, and M. Wyart, *Journal of Rheology* **60**, 905 (2016).
- [13] J. R. Royer, D. L. Blair, and S. D. Hudson, *Physical review letters* **116**, 188301 (2016).
- [14] C. Clavaud, A. Bérut, B. Metzger, and Y. Forterre, *Proceedings of the National Academy of Sciences*, 201703926 (2017).
- [15] J. Comtet, G. Chatté, A. Niguès, L. Bocquet, A. Siria, and A. Colin, *Nature communications* **8**, ncomms15633 (2017).
- [16] M. Liard, N. S. Martys, W. L. George, D. Lootens, and P. Hebraud, *Journal of Rheology* **58**, 1993 (2014).
- [17] Y. Madraki, S. Hormozi, G. Ovarlez, E. Guazzelli, and O. Pouliquen, *Physical Review Fluids* **2**, 033301 (2017).
- [18] C. D. Cwalina and N. J. Wagner, *Journal of Rheology* **60**, 47 (2016).
- [19] E. Brown, N. A. Forman, C. S. Orellana, H. Zhang, B. W. Maynor, D. E. Betts, J. M. DeSimone, and H. M. Jaeger, *arXiv preprint arXiv:0907.4999* (2009).
- [20] X. Chateau, G. Ovarlez, and K. L. Trung, *Journal of Rheology* **52**, 489 (2008).
- [21] F. Mahaut, X. Chateau, P. Coussot, and G. Ovarlez, *Journal of Rheology* **52**, 287 (2008).
- [22] F. Mahaut, *Comportement rhéologique de suspensions de particules non colloïdales plongées dans des fluides à seuil*, Ph.D. thesis, Paris Est (2009).
- [23] A. Fall, F. Bertrand, G. Ovarlez, and D. Bonn, *Journal of rheology* **56**, 575 (2012).
- [24] G. Ovarlez, F. Bertrand, and S. Rodts, *Journal of rheology* **50**, 259 (2006).
- [25] S. Dagois-Bohy, S. Hormozi, É. Guazzelli, and O. Pouliquen, *Journal of Fluid Mechanics* **776** (2015).
- [26] A. Poslinski, M. Ryan, R. Gupta, S. Seshadri, and F. Frechette, *Journal of Rheology* **32**, 703 (1988).
- [27] T.-S. Vu, G. Ovarlez, and X. Chateau, *Journal of Rheology* **54**, 815 (2010).
- [28] S. Asakura and F. Oosawa, *The Journal of Chemical Physics* **22**, 1255 (1954).
- [29] L. Onsager, *Annals of the New York Academy of Sciences* **51**, 627 (1949).
- [30] K. Zhao and T. G. Mason, *Physical review letters* **99**, 268301 (2007).
- [31] S. Sacanna, D. J. Pine, and G.-R. Yi, *Soft Matter* **9**, 8096 (2013).
- [32] C. W. Macosko, *Rheology: principles, measurements, and applications* (Wiley-vch, 1994).
- [33] G. Ovarlez, F. Mahaut, S. Deboeuf, N. Lenoir, S. Hormozi, and X. Chateau, *Journal of rheology* **59**, 1449 (2015).
- [34] M. Chow and C. Zukoski, *Journal of Rheology* **39**, 15 (1995).
- [35] X. Bian, S. Litvinov, M. Ellero, and N. J. Wagner, *Journal of Non-Newtonian Fluid Mechanics* **213**, 39 (2014).
- [36] P. Coussot, *Rheometry of pastes, suspensions, and granular materials: applications in industry and environment* (John Wiley & Sons, 2005).